Chinese Journal of Aeronautics, (2015),28(2): 535–544

Chinese Society of Aeronautics and Astronautics
& Beihang University

Chinese Journal of Aeronautics

cja@buaa.edu.cn
www.sciencedirect.com

A novel fault tolerant permanent magnet synchronous motor with improved optimal torque control for aerospace application

Guo Hong, Xu Jinquan *, Kuang Xiaolin

School of Automation Science and Electrical Engineering, Beihang University, Beijing 100191, China

Received 28 May 2014; revised 27 August 2014; accepted 3 November 2014
Available online 23 February 2015

KEYWORDS

Actuator;
Fault isolation;
Fault tolerant;
Optimal torque control;
Permanent magnet motor

Abstract Improving fault tolerant performance of permanent magnet synchronous motor has always been the central issue of the electrically supplied actuator for aerospace application. In this paper, a novel fault tolerant permanent magnet synchronous motor is proposed, which is characterized by two stators and two rotors on the same shaft with a circumferential displacement of mechanical angle of 4.5°. It helps to reduce the cogging torque. Each segment of the stator and the rotor can be considered as an 8-pole/10-slot five-phase permanent magnet synchronous motor with concentrated, single-layer and alternate teeth wound winding, which enhance the fault isolation capacity of the motor. Furthermore, the motor has high phase inductance to restrain the short-circuit current. In addition, an improved optimal torque control strategy is proposed to make the motor work well under the open-circuit fault and short-circuit fault conditions. Simulation and experiment results show that the proposed fault tolerant motor system has excellent fault tolerant capacity, which is able to operate continuously under the third open-circuit fault and second short-circuit fault condition without system performance degradation, which was not available earlier.

1. Introduction

With the development of power-by-wire (PBW) technology, the electrically supplied actuator has been the trend of servo-actuation system for aerospace application in the last decade,[1–3] due to the distinct advantage of replacing the centralized hydraulic system and eliminating all its associated disadvantages. In the past, the majority of the electrically supplied actuator can be divided into two categories: electro-hydrostatic actuator (EHA) and electro-mechanical actuator (EMA). There have been many successful applications, such as flight control surface actuators and fuel pumps[4] (for a survey, see, for example). Electrical machine system is the crucial part of the electrically supplied actuator, which determines the system performance of the servo-actuation system. Therefore, the electrical machine system with fault tolerant capacity has been the fundamental requirement in the aerospace application.

* Corresponding author. Tel.: +86 10 82339498.
E-mail address: xujinquan@buaa.edu.cn (J. Xu).
Peer review under responsibility of Editorial Committee of CJA.

Production and hosting by Elsevier

http://dx.doi.org/10.1016/j.cja.2015.01.008

Permanent magnet synchronous motor (PMSM) is widely used in servo-actuation system for aerospace application, due to the advantages of high power density and high efficiency.[5,6] However, the conventional three-phase PMSM has low armature magnetic field reconfiguration capacity and low fault isolation capacity, which cannot operate continuously under the fault condition. In order to meet the fault tolerant requirement of the PMSM in aerospace application, extensive research work has been reported on the fault tolerant PMSM (FTPMSM) design, which can be divided into two categories: the multiple sets of three-phase windings approach and the multiple single-phase windings approach.[4] For the multiple sets of three-phase windings approach, Bianchi et al.[7] proposed a dual three-phase PMSM, which is composed of two motors on the same shaft. Each motor is a three-phase PMSM. This FTPMSM can operate continuously with the first open-circuit fault. In Ref.[8], a FTPMSM with two sets of three-phase windings in the same stator is proposed. This FTPMSM cannot achieve the physical isolation between two sets of three-phase windings, and it is capable of continuous operation under the first open-circuit fault and short-circuit fault. In Ref.[9], a FTPMSM with four sets of three-phase windings is proposed, which consists of two motors on the same shaft. Each motor is a dual three-phase FTPMSM. This FTPMSM is able to operate continuously under the second open-circuit fault without system performance degradation. But this FTPMSM cannot operate continuously under the short-circuit fault, and it costs too much volume and weight, which is intolerable for the aerospace application. For the multiple single-phase windings approach, extensive research work has been reported on the four-phase, five-phase and six-phase FTPMSM with the fractional slot and concentrated windings[10–12] (for a survey, see, for example). This structure can improve the fault isolation capacity of the windings, and this FTPMSM is able to operate continuously under no more than the second open-circuit fault and short-circuit fault. However, in the practical engineering, this FTPMSM cannot guarantee the post-fault performance without system performance degradation under the fault condition. Since the current value of the remaining healthy phase windings for the FTPMSM under the fault condition will exceed the rated current value, the high current value will make the system overheat if the system still works without system degradation for long time. And the electromagnetic torque ripple will be larger under the second fault condition. Therefore, it is important to further explore the FTPMSM structure design to guarantee the post-fault performance without system performance degradation under the fault condition. Meanwhile, the control strategy for the FTPMSM is also one of the critical problems to be addressed urgently. Over the years, many important contributions have been made for the fault tolerant control of FTPMSM under the open-circuit fault and short-circuit fault, such as the optimal torque control in Refs.[13–15] and the optimal current control in Refs.[16–18] However, these fault control strategies cannot be applied for the FTPMSM with more than six-phase windings.

The scope of this paper falls into the FTPMSM system with the multiple single-phase windings approach. A novel FTPMSM, which can guarantee the post-fault performance under the third open-circuit fault and the second short-circuit fault without system performance degradation, is proposed in this paper.

2. FTPMSM design

PMSM is the crucial component of the electrically supplied actuator, which determines the system performance of the actuator. Therefore, it is vital to research the PMSM with high reliability. In this section, a novel FTPMSM is proposed as shown in Fig. 1. It is able to continually operate under the third open-circuit fault and the second short-circuit fault conditions. In addition, finite element analysis (FEA) of the electromagnetic field is adopted to analyze the characteristics of the proposed FTPMSM.

2.1. Structure design

In order to improve the fault tolerant capacity, the FTPMSM is characterized by two stators (stator 1 and stator 2) and two rotors (rotor 1 and rotor 2) on the same shaft with a circumferential displacement of 4.5° mechanical angle. Each set of the stator and the rotor can be considered as an 8-pole/10-slot five-phase PMSM with concentrated, single-layer and alternate teeth wound winding, as shown in Fig. 2. Here A, B, C, D, E denote the five-phase windings in each segment of the FTPMSM, and the subscript 1 denotes that these five-phase windings are located in stator 1 (similarly, the subscript 2 denotes that these five-phase windings are located in stator 2). This structure is able to guarantee the physical separation, magnetic isolation and thermal isolation of the windings. Therefore, when some of the phase windings are under the fault condition, the normal phase windings can still work well. This enhances the fault isolation of the windings. Furthermore, the electrical isolation capacity of the motor can be achieved via the use of H-bridge power supply. In addition, the two segments of the stator and the rotor have a difference of 4.5° mechanical angle, which is used to reduce the cogging torque of the developed FTPMSM. Since the phase windings' structure is fixed, the unequal-thickness permanent magnet is utilized to improve the sinusoidal waveform of back electromotive force.

To make the FTPMSM work well under the short-circuit fault condition, a phase inductance design approach is proposed to restrict the short circuit current. Let E_δ denotes the back electromotive force of the FTPMSM, R the phase resistance, L the phase inductance, and ω the angular frequency. When $R << \omega L$, the short circuit current I_s can be represented as

$$I_s \approx \frac{E_\delta}{\omega L} \tag{1}$$

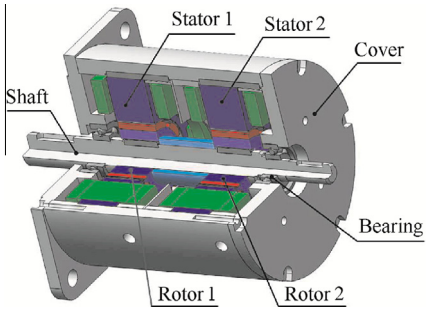

Fig. 1 Structure of the proposed FTPMSM.

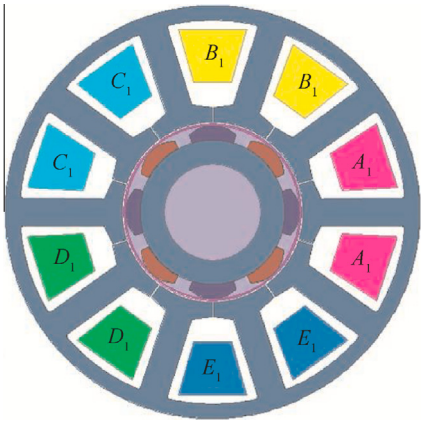

Fig. 2 Cross section of one segment of FTPMSM.

Since the FTPMSM phase inductance L consists of the synchronous inductance L_s, the harmonic leakage inductance L_h, the end-leakage inductance L_e and the slot leakage inductance L_{slot},[19] then

$$I_s < \frac{E_\delta}{\omega L_{slot}} \tag{2}$$

with

$$L_{slot} = \mu_0 N^2 l_{ef}\left(\frac{h_s}{3W_s} + \frac{h_0}{b_0}\right) \tag{3}$$

where μ_0 is the magnetic permeability, N the winding turns, l_{ef} the winding effective axial length, h_s the slot height, W_s the slot width, h_0 the slot opening height, and b_0 the slot opening width. Therefore, the short circuit current I_s will decrease as the increase of the slot leakage inductance L_{slot}. That is, with the slot shape design, the desired phase inductance can be obtained easily. In this paper, the magnitude of short circuit current is restrained at the rated current value.

2.2. Electromagnetic FEA

Previous analysis has shown the structure design of the proposed FTPMSM. In this section, the electromagnetic FEA of the FTPMSM is conducted to verify the design approach. Due to the axial symmetry of the FTPMSM, a two dimensional (2-D) finite element model is employed in the FEA. And the FTPMSM design specification is listed in Table 1. Note that any segment of the FTPMSM is designed to meet the design specification, which is able to guarantee the developed FTPMSM to work well under the fault condition without system performance degradation.

Table 1 Design specification of FTPMSM.

Parameter	Value
Supply voltage (V)	28
Rated power (W)	200
Rated speed (r/min)	6000
Rated torque (N·m)	0.3
Rated current (A)	5
Short-circuit current (A)	5

Fig. 3 shows the magnetic flux line of the FTPMSM with no load, in which A denotes the magnetic vector potential. Note that there is almost no magnetic flux line coupling between the phase windings. Fig. 4 shows the magnetic flux density of the FTPMSM under rated load condition, in which B denotes the magnetic flux density. The maximum magnetic flux density is 1.6 T, located in the stator yoke, which does not exceed the saturation value of the silicon steel sheet. Fig. 5 shows the magnetic flux density of the FTPMSM under the extreme condition that all the phase windings are in short-circuit fault.

Fig. 6 is the magnification of Fig. 5. The minimum magnetic flux density in the magnets is 0.4 T, which means that

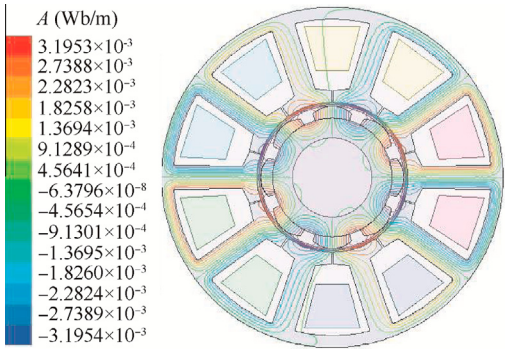

Fig. 3 Magnetic flux line of FTPMSM with no load.

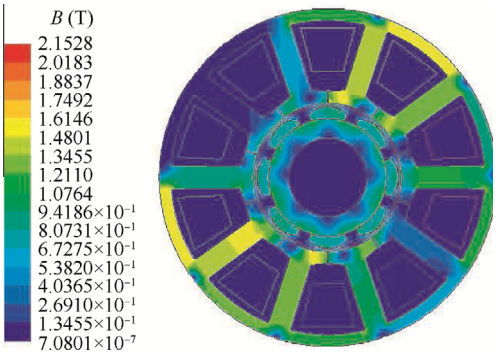

Fig. 4 Magnetic flux density of FTPMSM with rated load.

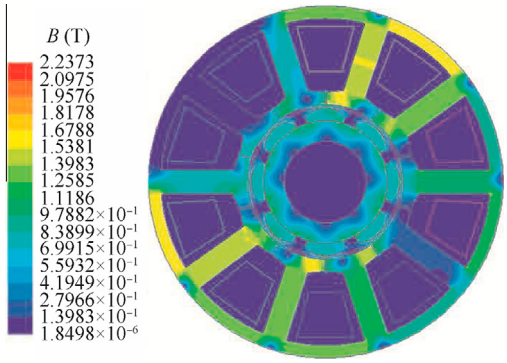

Fig. 5 Magnetic flux density of FTPMSM with short-circuit fault.

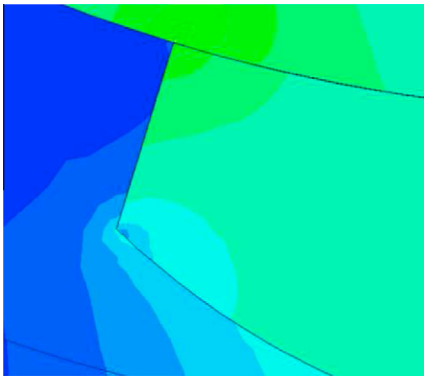

Fig. 6 Magnification of Fig. 5.

the magnets are not demagnetized. Fig. 7 shows one-phase back electromotive force at the rated speed of 6000 r/min. The waveform of the back electromotive force is almost sinusoidal. Fig. 8 shows the phase self-inductance of the FTPMSM. The phase self-inductance is approximately 1.33 mH, which means the short circuit current can be limited in the desired range. Fig. 9 shows the phase mutual inductance of the FTPMSM. It equals to almost zero, that is, the FTPMSM has great magnetic isolation capacity.

According to the design, the proposed FTPMSM has high fault isolation capacity. To achieve the fault tolerant capacity of the FTPMSM system, the corresponding control strategy

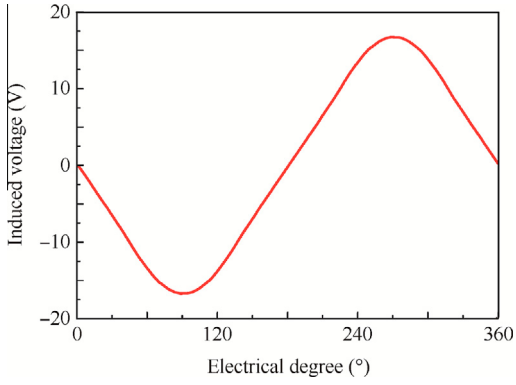

Fig. 7 One-phase back electromotive force of FTPMSM at 6000 r/min.

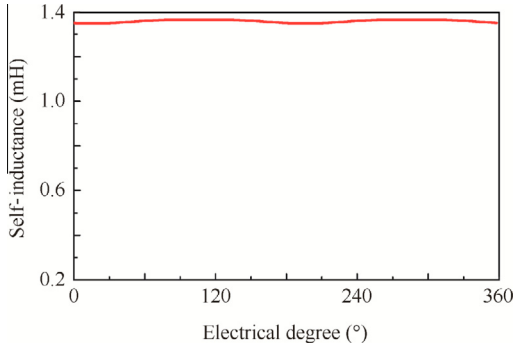

Fig. 8 Self-inductance of FTPMSM.

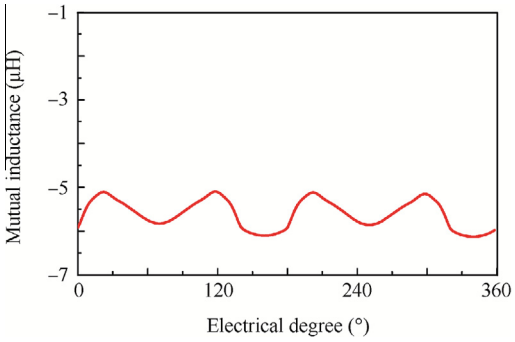

Fig. 9 Mutual inductance of FTPMSM.

must be involved, which is able to make the system work well via the use of the rest healthy phase windings when some of the phase windings are faulted. In next section, we will further explore the control strategy for the proposed FTPMSM.

3. Control strategy

Only with the proper fault control strategy, the developed FTPMSM can achieve the post-fault operation after the fault occurrence. In this section, a cascaded dual closed loop control structure is adopted, including the speed loop and the current loop. Moreover, an improved optimal torque control strategy is proposed to formulate the required current command for the current loop. And the block diagram of the dual closed-loop control structure is shown in Fig. 10, where ω_{ref} denotes the speed command signal, ω_{back} the speed feedback signal, T_{ref} the electromagnetic torque command signal, θ_{back} the rotor angle signal, I_{ref} the current command signal, I_{back} the current feedback signal, and U_{ref} the voltage command signal.

3.1. Improved optimal torque control

To achieve the continuous operation of the FTPMSM under the conditions of both open-circuit and short-circuit fault, the improved optimal torque control is proposed by formulating the calculation of the electromagnetic torque as a constrained optimization problem, which can generate a smooth electromagnetic torque while minimizing the copper losses. The essence of the improved optimal torque control is to compensate the impact of the fault via the use of the remaining healthy phase winding.

For the developed FTPMSM, the instantaneous electromagnetic torque can be represented as

$$T_{\text{e}} = \sum_{j=1}^{10} K_j I_j \tag{4}$$

where T_{e} is the instantaneous electromagnetic torque; K_j is the back electromotive force coefficient, which is equal to the instantaneous ratio of the phase back electromotive force to the rotor speed; I_j is the instantaneous phase current. Then the instantaneous electromagnetic torque of the developed FTPMSM under the fault condition can be represented as

$$T_{\text{e}} = \sum_{j \neq k_i}^{10} K_j I_j + T_{\text{r}} \tag{5}$$

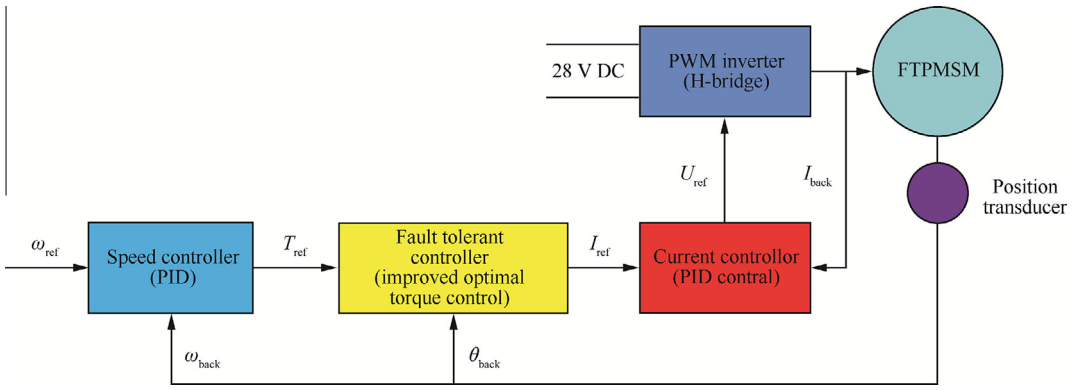

Fig. 10 Dual closed-loop control structure.

with

$$T_r = \sum_{i=1}^{n} K_{k_i} I_{k_i} \tag{6}$$

where T_r is the electromagnetic torque caused by the faulted phase; k_i denotes the faulted k_ith phase, with $n \in [0,4]$ the total faulted phase. Note that for the open-circuit fault condition, $T_r = 0$ as $I_{k_i} = 0$. Then the constrained optimization problem can be formulated as

$$\min R\sum_{j=1}^{10} I_j^2 \tag{7}$$

which is subject to the constraint of Eq. (5). The optimization problem can be solved by minimizing the augmented objective function $F(I_1, I_2, \ldots, I_{10}, \lambda)$[20]

$$F = \sum_{j=1}^{10} I_j^2 + \lambda\left(T_e - T_r - \sum_{j\neq k_i}^{10} K_j I_j\right) \tag{8}$$

where λ is the Lagrange multiplier. For $i = 1, 2,\ldots,n$ and $j \neq k_i$, taking the derivative of F with respect to I_j, we can have

$$\frac{\partial F}{\partial I_j} = 2I_j - \lambda K_j \tag{9}$$

Taking the derivative of F with respect to λ yields

$$\frac{\partial F}{\partial \lambda} = T_e - T_r - \sum_{j\neq k_i}^{10} K_j I_j \tag{10}$$

For $i = 1, 2,\ldots,n$ and $j \neq k_i$, let

$$\frac{\partial F}{\partial I_j} = 0 \tag{11}$$

and

$$\frac{\partial F}{\partial \lambda} = 0 \tag{12}$$

Then the instantaneous phase current command in the healthy phase can be given by

$$I_j = (T_e - T_r)\frac{K_j}{\sum_{j\neq k_i}^{10} K_j^2} \tag{13}$$

The optimal torque control is an instantaneous torque control strategy. In addition, under the fault condition, this approach will result in significant time harmonics in the healthy phase current.

3.2. Fault mode analysis

In order to study the fault tolerant performance of the developed FTPMSM, it is important to analyze the fault mode of the FTPMSM, which will provide a guideline for engineers to follow when the FTPMSM is implemented. According to the structure of the proposed FTPMSM, the fault mode of the system is summarized as follows:

(1) First fault: there is one-phase winding of the FTPMSM with fault, including the open-circuit fault and the short-circuit fault.
(2) Second fault: there are two-phase windings of the FTPMSM with fault, including the open-circuit fault and the short-circuit fault.
(3) Third fault: there are three-phase windings of the FTPMSM with fault, including the open-circuit fault and the short-circuit fault.

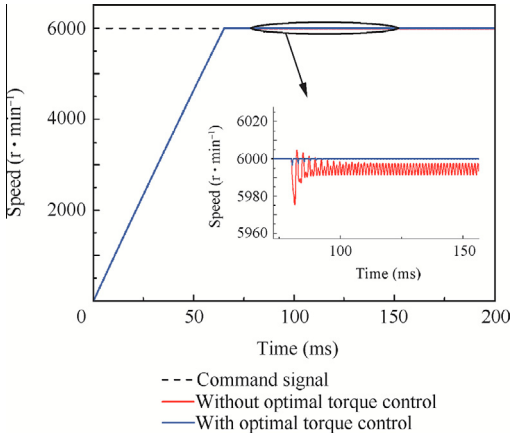

Fig. 11 Speed step response of the developed FTPMSM system with the second short-circuit fault.

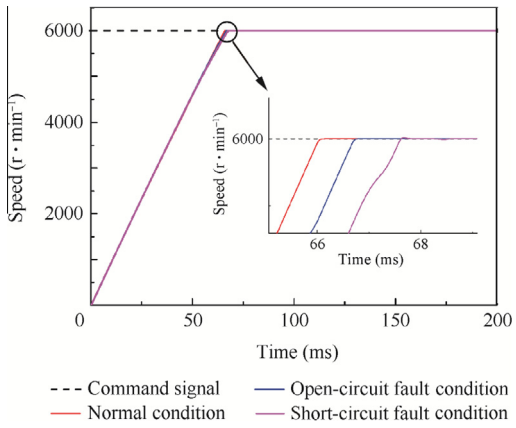

Fig. 12 Speed step response of the developed FTPMSM system with the third open-circuit fault and the second short-circuit fault.

(4) Fourth fault: there are four-phase windings of the FTPMSM with fault, including the open-circuit fault and the short-circuit fault.
(5) Fifth fault: there is five-phase windings of the FTPMSM with fault, including the open-circuit fault and the short-circuit fault.

Similarly, we can also obtain the fault modes of the sixth fault, the seventh fault and the eighth fault.

3.3. System simulation

The computer simulation is conducted to verify the fault control strategy in this section. We assume that the current root mean square (RMS) value of the developed FTPMSM under the fault condition cannot exceed the rated current RMS value, which can guarantee that the system can operate continuously under long-time duty without system performance degradation. Fig. 11 shows the speed step response of the developed FTPMSM system at rated load under the second short-circuit fault condition for both with the optimal control and without the control, in which we take the fault phase windings (A_1, A_2) for example. With the improved optimal torque control, the developed FTPMSM can work well under the second short-circuit fault condition, while the speed trajectory of the FTPMSM fluctuates below the command signal without the optimal torque control. Fig. 12 shows the speed step response of the developed FTPMSM with the improved optimal torque control under the third open-circuit fault and the second short-circuit fault condition. Here the fault phase windings of third open-circuit fault are (A_1, A_2, C_1), which is the worst condition for the third open-circuit fault. Similarly, the

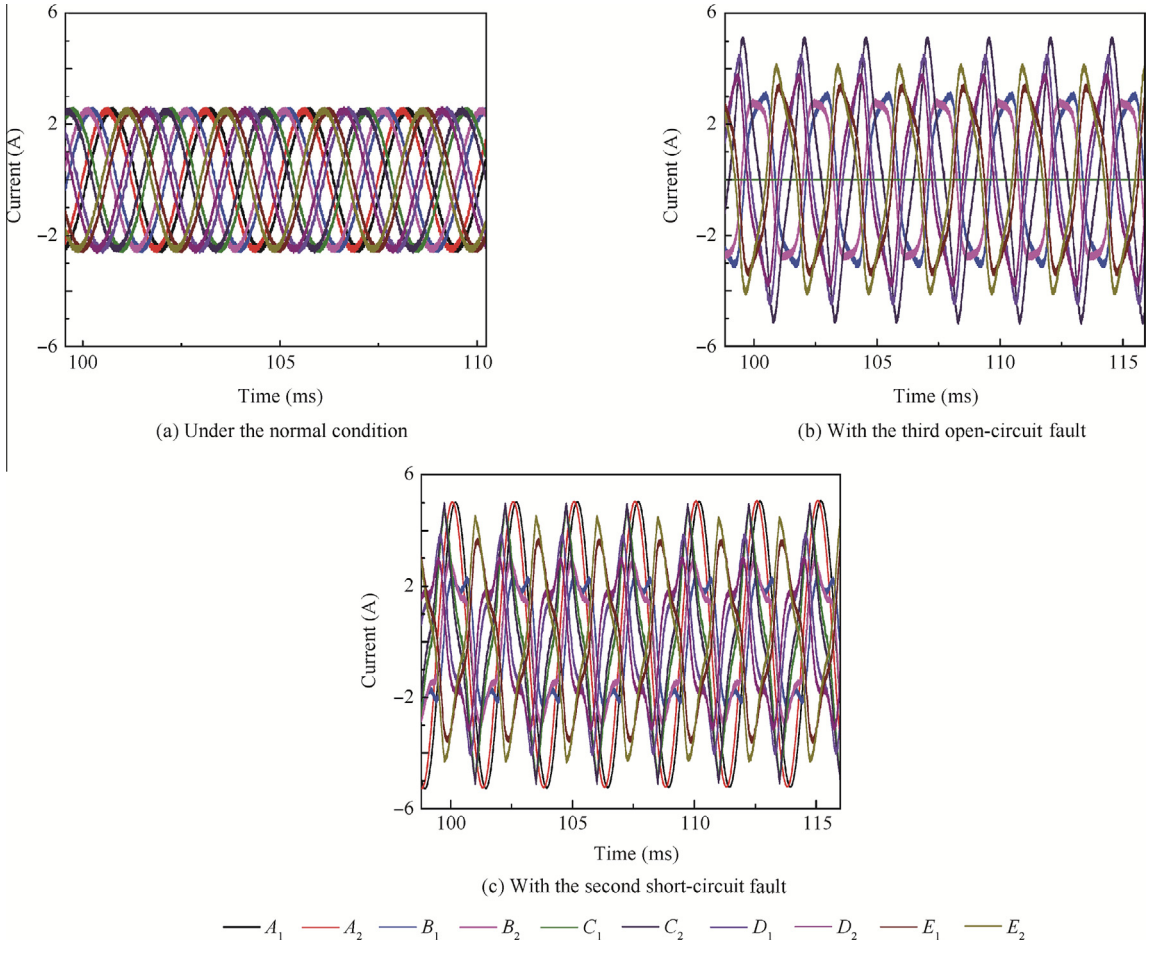

Fig. 13 Current waveform of the proposed FTPMSM.

fault phase windings of second short-circuit fault are (A_1, A_2). Note that the settling time of the developed FTPMSM system is 66.1 ms for the normal condition, 66.8 ms for the open-circuit fault condition and 67.8 ms for the short-circuit fault condition. After that, the controlled trajectories of the system under both the open-circuit fault and the short-circuit conditions stay around 6000 r/min. That is, the FTPMSM system can work well under the third open-circuit fault and second short-circuit fault. Fig. 13 shows the current of the developed FTPMSM under normal, the third open-circuit fault and the second short-circuit fault conditions. For the FTPMSM system under the third open-circuit fault and the second short-circuit fault conditions, the current RMS value is no more than the rated current RMS value. Therefore, the developed FTPMSM system is able to operate continuously under the third open-circuit fault and the second short-circuit fault without system performance degradation.

Fig. 14 shows the speed step response of the developed FTPMSM at rated load with the fourth open-circuit fault and the third short-circuit fault. Here the fault windings of fourth open-circuit fault are (A_1, A_2, C_1, C_2), while the fault windings of third short-circuit fault are (A_1, A_2, C_1). Fig. 15 shows the current of the developed FTPMSM with fourth open-circuit fault and the third short-circuit fault conditions, respectively. Although the developed system with both the open-circuit fault and short-circuit fault can keep in good response, the current RMS values of the system with both open-circuit fault and short-circuit fault exceed the rated current RMS value, which will make the system overheat if the FTPMSM system still operates under the long-time duty. That is, the developed FTPMSM system has to operate with system performance degradation under the fourth open-circuit fault and the third short-circuit fault condition.

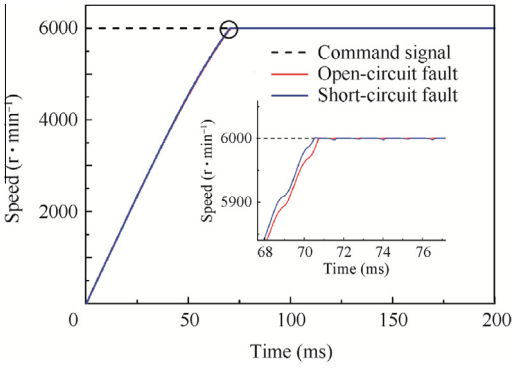

Fig. 14 Speed step response of the developed FTPMSM system with the fourth open-circuit fault and the third short-circuit fault.

4. Experimental validation

To verify the fault tolerant performance, the developed FTPMSM is prototyped, and the experimental setup is built, as shown in Fig. 16. The developed FTPMSM system consists of microprocessor control unit (MCU), power drive unit (PDU), signal detection and processing unit (SDPU) and the FTPMSM. The MCU, based on digital signal processor (DSP) TMS320F2812 and field programmable gate array (FPGA) EP2C35F484, is used to receive the control command and feedback signal and accomplish the control algorithm, and control the PDU and SDPU. The PDU adopts the H-bridge converter to supply electric power for the FTPMSM. And the SDPU is composed of Hall current sensor, analog-to-digital converter AD7607, and resolver-to-digital converter AD2S1210. It is used to convert the analog signal (speed, position and phase current) into the digital signal for the MCU.

First, the experiments of the developed FTPMSM system under the normal condition are performed. The sample rates for the speed loop and the current loop are 100 μs and 25 μs, respectively. The rated load torque is 0.3 N·m. Fig. 17 shows the speed sinusoidal response of the developed FTPMSM system at 20 Hz with no load. The phase lag of the speed response is 74.9°, and there is almost no amplitude attenuation. Fig. 18 shows the speed sinusoidal response of the developed FTPMSM system at 10 Hz with full load. The phase lag of the speed response is 51.8°, while the amplitude attenuation is 0.26 dB.

Next, the experiments of the developed system under the third open-circuit fault and the second short-circuit fault conditions are conducted. Here we take the fault windings (A_1, A_2, C_1) for third open-circuit fault, and (A_1, A_2) for second short-circuit fault for example. Fig. 19(a) shows the C_2-phase current

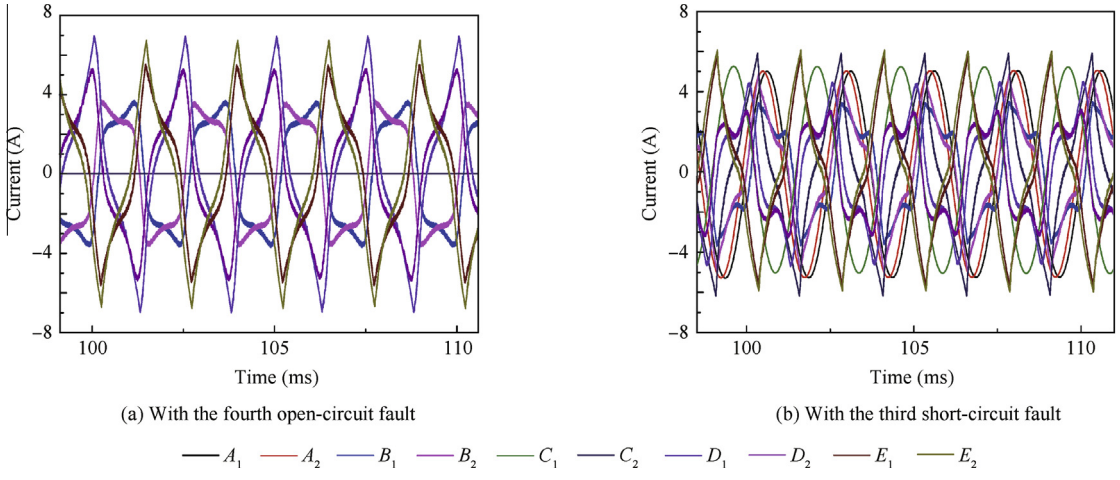

Fig. 15 Current waveform of the proposed FTPMSM.

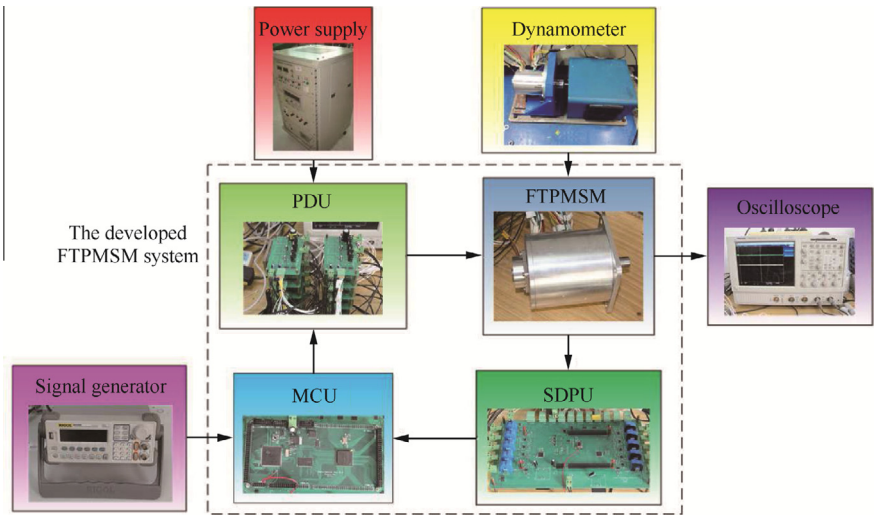

Fig. 16 Experimental setup of the developed FTPMSM.

of the developed FTPMSM under the third open-circuit fault at rated speed 6000 r/min, which has the maximum phase current in all the remaining healthy windings. Although the peak value (7 A) of phase current exceeds the rated value (5 A), the RMS value of phase current is no more than the rated RMS value. Fig. 19(b) shows the electromagnetic torque of the developed FTPMSM with the third open-circuit fault. The electromagnetic torque of the developed FTPMSM with third open-circuit fault is almost the same as that under the normal condition. Fig. 20(a) shows the C_2-phase current of the developed FTPMSM with the second short-circuit fault at rated speed 6000 r/min, which has the maximum phase current in all the remaining healthy windings. Under second short-circuit fault, the phase current of the FTPMSM does not exceed the rated value. Fig. 20(b) shows the electromagnetic torque of the developed FTPMSM with the second short-circuit fault. Note that the electromagnetic torque with the second short-circuit fault is as well as that in the normal condition. As a result,

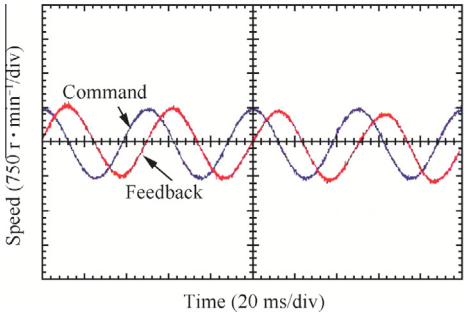

Fig. 17 Speed sinusoidal response at 20 Hz with no load.

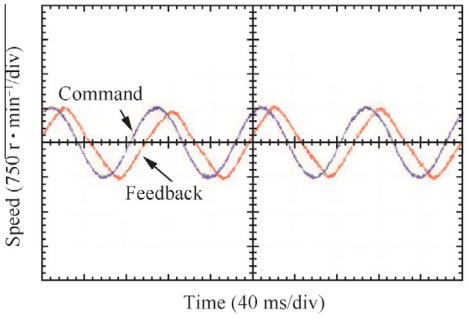

Fig. 18 Speed sinusoidal response at 10 Hz with full load.

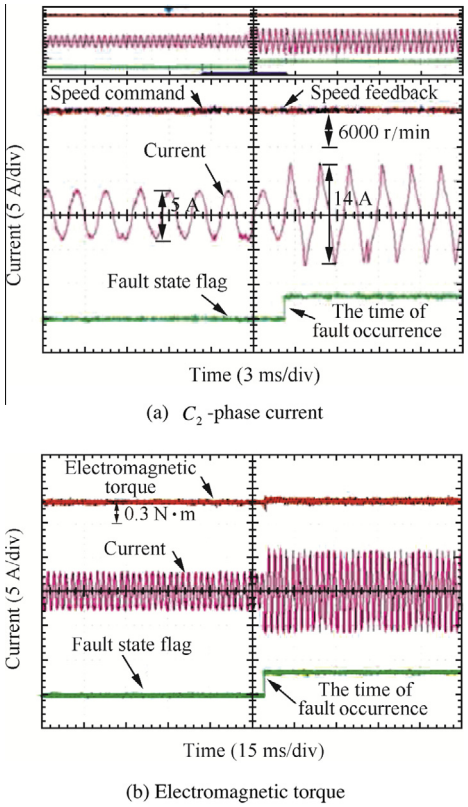

Fig. 19 C_2-phase current and electromagnetic torque of the developed FTPMSM with the third open-circuit fault.

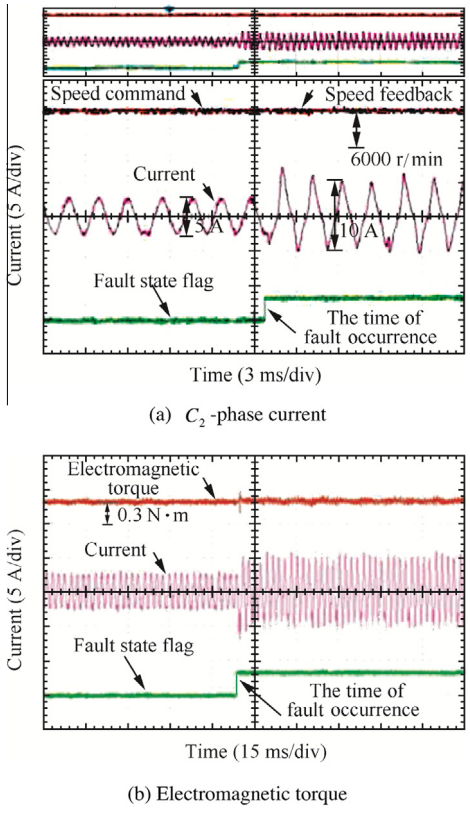

Fig. 20 C_2-phase current and electromagnetic torque of the developed FTPMSM with the second short-circuit fault.

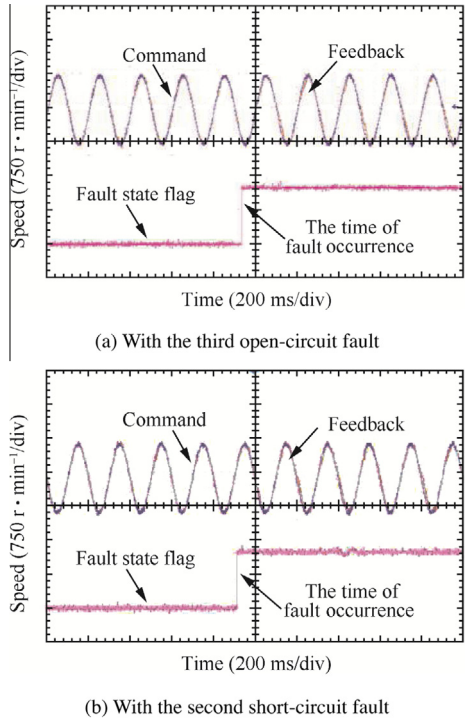

Fig. 21 Speed sinusoidal response at 5 Hz with the third open-circuit fault and the second short-circuit fault.

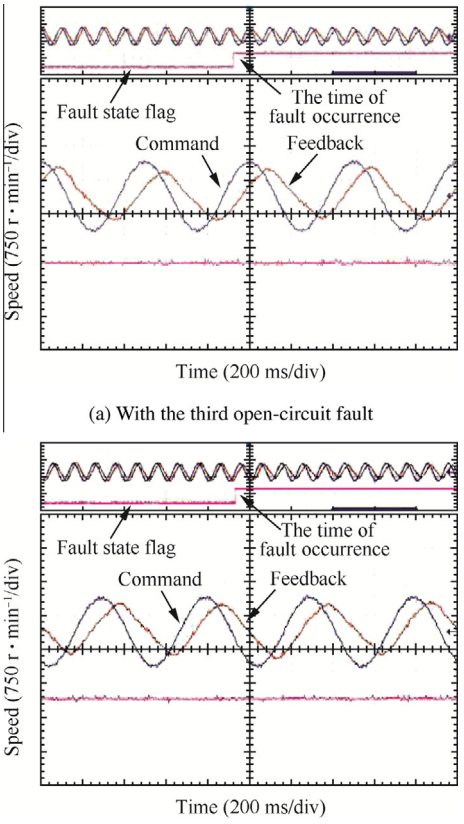

Fig. 22 Speed sinusoidal response at 10 Hz with the third open-circuit fault and the second short-circuit fault.

the improved optimal torque control can guarantee the ripple-free torque operation of the proposed FTPMSM with the open-circuit fault and the short-circuit fault.

Fig. 21(a) shows the speed sinusoidal response of the developed FTPMSM system at 5 Hz with full load with the third open-circuit fault. Fig. 21(b) shows the speed sinusoidal response of the developed FTPMSM system at 5 Hz with full load under the second short-circuit fault. The results show that there is almost no system performance degradation after the fault occurrence, that is, the developed FTPMSM has excellent fault tolerant capacity.

Fig. 22(a) shows the speed sinusoidal response of the developed FTPMSM system at 10 Hz with full load with the third open-circuit fault. Fig. 22(b) shows the speed sinusoidal response of the developed FTPMSM system at 10 Hz with full load with the second short-circuit fault. The phase lag of the speed response for the developed FTPMSM system under the open-circuit fault is 83.5°, while the amplitude attenuation for the system is 2.5 dB. And the phase lag of the speed response for the developed FTPMSM system with the short-circuit fault is 77.7°, while the amplitude attenuation is 2 dB. Therefore, the speed bandwidth of the developed FTPMSM system with the third open-circuit fault and the second short-circuit fault is still able to achieve 10 Hz.

5. Conclusions

(1) A novel FTPMSM is proposed, which is characterized by two stators and two rotors on the same shaft with a circumferential displacement of mechanical angle of 4.5°. With the concentrated, single-layer and alternate teeth wound winding, the motor has outstanding fault isolation capacity. And the FTPMSM can effectively restrain the short-circuit current by the high phase inductance.
(2) The improved optimal torque control strategy is proposed, which is able to make the ten-phase FTPMSM work well with the open-circuit and short-circuit fault.
(3) The simulation and experiment results show that the developed FTPMSM system is able to operate continuously under the third open-circuit fault and the second short-circuit fault without system performance degradation. Moreover, the speed bandwidth of the system with the third open-circuit fault and the second short-circuit fault is still able to achieve 10 Hz.

Future exploration in the transient process after the fault occurrence of the developed FTPMSM system is also interesting and worth pursuing.

References

1. Bennett JW, Atkinson GJ, Mecrow BC, Atkinson DJ. Fault-tolerant design considerations and control strategies for aerospace drives. *IEEE Trans Ind Electron* 2012;**59**(5):2049–58.
2. Naidu M, Gopalakrishnan S, Nehl T. Fault-tolerant permanent magnet motor drive topologies for automotive x-by-wire systems. *IEEE Trans Ind Appl* 2010;**46**(2):841–8.
3. Kang RJ, Jiao ZX, Wang SP, Chen LS. Design and simulation of electro-hydrostatic actuator with a built-in power regulator. *Chin J Aeronaut* 2009;**22**(6):700–6.
4. Cao WP, Mecrow BC, Atkinson GJ, Bennett JW, Atkinson DJ. Overview of electric motor technologies used for more electric aircraft (MEA). *IEEE Trans Ind Electron* 2012;**59**(9):3523–31.
5. Mecrow BC, Jack AG, Haylock JA, Coles J. Fault-tolerant permanent magnet machine drives. *Electr Mach Drives* 1996;**143**(6):437–42.
6. Jack AG, Mecrow BC, Haylock JA. A comparative study of permanent magnet and switched reluctance motors for high-performance fault-tolerant applications. *IEEE Trans Ind Appl* 1996;**32**(4):889–95.
7. Bianchi N, Dai Pre M, Bolognani S. Design of a fault-tolerant IPM motor for electric power steering. *IEEE Trans Veh Technol* 2006;**55**(4):1102–11.
8. Guo H, Wang W, Xing W, Li YM. Design of electrical/mechanical hybrid 4-reduncancy brushless DC torque motor. *Chin J Aeronaut* 2010;**23**(2):211–5.
9. Vaseghi B, Takorabet N, Caron JP, Nahid-Mobarakeh B, Meibody-Tabar F, Humbert G. Study of different architectures of fault-tolerant actuator using a two-channel PM motor. *IEEE Trans Ind Appl* 2011;**47**(1):47–54.
10. EI-Refaie AM. Fault-tolerant permanent magnet machines: a review. *IET Electr Power Appl* 2011;**5**(1):59–74.
11. Dwari S, Parsa L. Fault-tolerant control of five-phase permanent magnet motors with trapezoidal back EMF. *IEEE Trans Ind Electron* 2011;**58**(2):476–85.
12. Bianchi N, Bolognani S, Dai Pre M. Impact of stator winding of five-phase permanent magnet motor on postfault operations. *IEEE Trans Ind Electron* 2008;**55**(5):1978–87.
13. Ede JD, Atallah K, Wang JB, Howe D. Effect of optimal torque control on rotor loss of fault-tolerant permanent-magnet brushless machines. *IEEE Trans Magn* 2002;**38**(5):3291–3.
14. Wang JB, Atallah K, Howe D. Optimal torque control of fault-tolerant permanent magnet brushless machines. *IEEE Trans Magn* 2003;**39**(5):2962–4.
15. Sun ZG, Wang JB, Jewell GW, Howe D. Enhanced optimal torque control of fault-tolerant PM machine under flux-weakening operation. *IEEE Trans Ind Electron* 2010;**57**(1):344–53.
16. Mohammadpour A, Sadeghi S, Parsa L. A generalized fault-tolerant control strategy for five-phase PM motor drives considering star, pentagon, and pentacle connections of stator windings. *IEEE Trans Ind Electron* 2014;**61**(1):63–75.
17. Bianchi N, Bolognani S, Dai Pre M. Strategies for the fault-tolerant current control of a five-phase permanent-magnet motor. *IEEE Trans Ind Appl* 2007;**43**(4):960–70.
18. Zhao WX, Chau KT, Cheng M, Ji JH, Zhu XY. Remedial brushless AC operation of fault-tolerant doubly salient permanent-magnet motor drives. *IEEE Trans Ind Electron* 2010;**57**(6):2134–41.
19. EI-Refaie AM, Zhu ZQ, Jahns TM, Howe D. Winding inductances of fractional slot surface-mounted permanent magnet brushless machines. *Int J Comput Math Electr Electron Eng* 2009;**28**(6):1590–606.
20. Bertsekas DP. *Nonlinear programming*. Massachusetts: Athena Scientific Press; 1999. p. 275–368.

Guo Hong is a professor and Ph.D. supervisor at School of Automation Science and Electrical Engineering, Beihang University. His research interests include the design and control of permanent magnet motor, robust design theory of electrical machine and design theory of electrical machine with high reliability.

Xu Jinquan is a Ph.D. student at School of Automation Science and Electrical Engineering, Beihang University. He received his B.S. degree from Beihang University in 2009. His area of research includes fault tolerant permanent magnet motor design, fault tolerant control and robust control.

Kuang Xiaolin is a Ph.D. student at School of Automation Science and Electrical Engineering, Beihang University. He received his B.S. degree from Beihang University in 2012. His area of research includes airborne power distribution system, redundancy management, motor design and control.